JACS
JOURNAL OF THE AMERICAN CHEMICAL SOCIETY
Article
pubs.acs.org/JACS

Rationally Designed Small Molecules That Target Both the DNA and RNA Causing Myotonic Dystrophy Type 1

Lien Nguyen,[†] Long M. Luu,[†] Shaohong Peng,[‡] Julio F. Serrano,[†] H. Y. Edwin Chan,[‡] and Steven C. Zimmerman*[,†]

[†]Department of Chemistry, University of Illinois at Urbana—Champaign, 600 South Mathews Avenue, Urbana, Illinois 61801, United States

[‡]Laboratory of Drosophila Research and School of Life Sciences, The Chinese University of Hong Kong, Shatin N.T., Hong Kong, SAR

Supporting Information

ABSTRACT: Single-agent, single-target therapeutic approaches are often limited by a complex disease pathobiology. We report rationally designed, multi-target agents for myotonic dystrophy type 1 (DM1). DM1 originates in an abnormal expansion of CTG repeats (CTG^{exp}) in the *DMPK* gene. The resultant expanded CUG transcript (CUG^{exp}) identified as a toxic agent sequesters important proteins, such as muscleblind-like proteins (MBNL), undergoes repeat-associated non-ATG (RAN) translation, and potentially causes microRNA dysregulation. We report rationally designed small molecules that target the DM1 pathobiology *in vitro* in three distinct ways by acting simultaneously as transcription inhibitors, by inhibiting aberrant protein binding to the toxic RNA, and by acting as RNase mimics to degrade the toxic RNA. *In vitro*, the agents are shown to (1) bind CTG^{exp} and inhibit formation of the CUG^{exp} transcript, (2) bind CUG^{exp} and inhibit sequestration of MBNL1, and (3) cleave CUG^{exp} in an RNase-like manner. The most potent compounds are capable of reducing the levels of CUG^{exp} in DM1 model cells, and one reverses two separate CUG^{exp}-induced phenotypes in a DM1 *Drosophila* model.

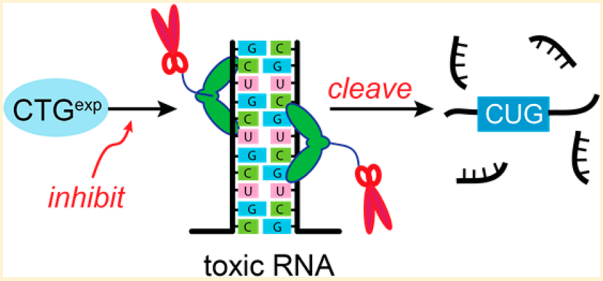

INTRODUCTION

Drug discovery efforts traditionally place a high premium on agents that operate on a single target with high selectivity and affinity. However, rapid advances in "omics" have revealed the complexity of many diseases, especially cancer, where as many as 500 gene products may be disregulated.[1] In such cases, a "magic bullet" approach may be quite limited. Indeed, studies have suggested that in at least some cases less selective drugs exerting their pharmacologic effect on multiple targets can be superior to those with narrow activity profiles.[2] These realizations have led some to suggest a paradigm shift from "single drug, single target" to polypharmacologic or multi-target drug discovery (MTDD) approaches.[2,3] The main challenge in MTDD is the need to design a drug that modulates multiple disease targets simultaneously. Especially difficult is creating fused, hybrid structures whose different molecular segments recognize different targets. A much simpler strategy is to tether together two or more structural domains with different biological activities.[4,5] These multiple ligands may be conjugates of two known inhibitors (e.g., of two signaling pathways) or a binding unit and a chemically reactive group.

Although MTDD efforts have largely focused on protein targets, the increasing importance of RNA as a therapeutic target makes it an excellent candidate for MTDD. We were particularly attracted to myotonic dystrophy type 1 (DM1) because its complicated disease pathogenesis is increasingly well-understood, providing well-defined DNA, RNA, and protein targets for a small-molecule MTDD approach. DM1 is an incurable, multisystemic neuromuscular disease that is caused by an abnormal expansion of the CTG trinucleotide repeats (CTG^{exp}) in the 3′-untranslated region of the *DMPK* gene on chromosome *19q13* (see Figure 1a, top box).[6] This expanded DNA, which can reach 50−2000 CTG repeats, yields an expanded CUG RNA transcript (CUG^{exp}) that sequesters the alternative-splicing regulator muscleblind-like protein (MBNL), leading to splicing defects and disease symptoms.

We and others have developed small molecules that inhibit the MBNL1 sequestration by CUG^{exp}.[7−14] However, a recently expanded view of DM1 pathogenesis has suggested that additional CUG^{exp}-induced toxic pathways must be considered for the disease phenotype to be fully reversed. In particular, the CTG·CAG repeats undergo bidirectional transcription, producing two transcripts, CUG^{exp} and CAG^{exp},[15,16] that both undergo repeat-associated non-ATG (RAN) translation, generating multiple toxic homopeptides.[17,18] Further, it was shown that CUG^{exp} disrupted the translation of the MEF2 protein, which affects multiple levels of mRNA and microRNA

Received: September 5, 2015
Published: October 16, 2015

DOI: 10.1021/jacs.5b09266
J. Am. Chem. Soc. 2015, 137, 14180−14189

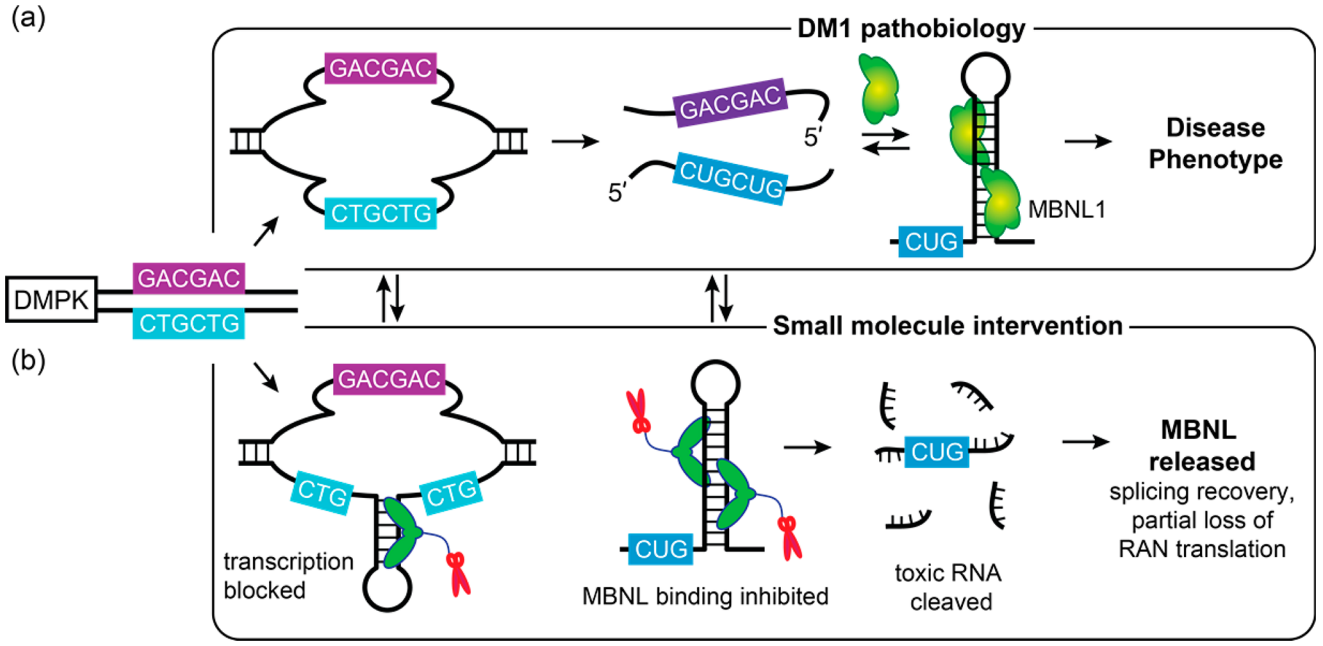

Figure 1. Schematic illustration of DM1 pathobiology and multi-target treatment. (a) RNA gain-of-function disease pathogenesis. The expanded DNA trinucleotide repeat (CTG^{exp}) undergoes transcription to form a CUG^{exp} hairpin that sequesters MBNL proteins (e.g., MBNL1). The MBNL level depletion causes splicing defects of more than 100 pre-mRNAs, resulting in disease symptoms. RAN translation of CUG^{exp} and CAG^{exp} generates toxic homopeptides. (b) Small-molecule intervention. Small molecules (green) target the CTG^{exp} hairpin, inhibiting production of CUG^{exp}. Any CUG^{exp} formed is bound by small molecules, inhibiting MBNL and other protein sequestration. Cleaving functionality (red) processes the toxic RNA. All three small-molecule interventions free MBNL for its normal function. Likewise, other toxic pathways induced by the CUG^{exp} are eliminated.

in human DM1 heart tissues.[19] Furthermore, the discovery of other proteins involved in the formation of MBNL1–CUG^{exp} foci suggests that other toxic pathways may be induced by CUG^{exp}.[20,21]

The studies above suggest that a multi-target drug approach, especially one that degrades the toxic CUG^{exp} or inhibits its formation, may be more effective. Agents that perform one of these two functions are known. Thus, Cooper[22] and Thornton[23] reported antisense agents that induce CUG^{exp} cleavage via an RNase H-mediated mechanism and are currently in clinical trials, and Disney developed a small molecule that photodegrades the toxic transcript.[24] Analogues of pentamidine were reported by Berglund to inhibit the synthesis of CUG^{exp} by binding to the $(CTG{\cdot}CAG)_n$ duplex.[25] We report herein a rational MTDD effort leading to small molecules that intervene in three separate steps in the DM1 pathobiology, suppressing CUG^{exp} mRNA levels and reversing the disease phenotype in DM1 model cells and a DM1 *Drosophila* model.

RESULTS AND DISCUSSION

Multi-target Ligand Design. Our overall approach was to develop agents able to intervene in the DM1 pathogenic mechanism in three ways: (1) targeting CTG^{exp} to inhibit its transcription to CUG^{exp}, (2) targeting CUG^{exp} to inhibit MBNL1 sequestration, and (3) hydrolytically degrading the CUG^{exp} with RNase-like catalytic functionality (see Figure 1b, bottom box). We previously reported two classes of rationally designed agents (e.g., **1** and **2**) that selectively bound CUG^{exp} and inhibited MBNL binding with low micromolar K_I values.[11,12,26] Both ligands feature triaminotriazine moieties to recognize the UU mismatch in duplex CUG^{exp} and provide sequence selectivity, whereas the acridine group in **1** and the bisamidinium unit in **2** were selected to drive the association by A-form RNA intercalation and groove binding, respectively. Although **1** was not cell-permeable, analogue **3** utilized the polyamine transport system to enter cells.[27,28] The bisamidinium unit in **2** was chosen partly because it was reported to localize in cell nuclei; indeed, both **2** and **3** dissolved the MBNL1–CUG^{exp} nuclear foci and partially rescued splicing defects of *IR* and *cTNT* minigenes in DM1 model cell cultures (Chart 1).[12,27]

In comparison to **1**, bisamidinium-containing **2** showed similar *in vitro* inhibition potency, but with lower toxicity, higher water solubility, and better cell uptake. Nonetheless, the acridine ligands are inherently multi-targeting because of their ability to bind both the DNA and RNA causing DM1. Thus, agent **1** complexes an oligonucleotide 10-mer containing a single dCTG and rCUG site with the binding constant K_D = 0.39 and 0.43 nM, respectively.[11] In contrast, agent **2** is selective for CUG^{exp}, showing no detectable binding of dCTG by isothermal titration calorimetry (ITC) (vide infra). Beyond their ability to inhibit the sequestration of MBNL and other proteins, both **1** and **2** have the potential to become CUG^{exp} cleaving agents with attachment of suitable functionality.

Numerous small-molecule mimics of RNase A were developed over the past few decades.[29,30] Many use the active-site functional groups found in RNase A in an effort to mimic its well-established acid–base mechanism of action.[31] Although none of the mimics cleaved RNA as effectively as RNase A, those containing at least one ammonium ion and an imidazole or amino group were the most promising. Based on this information, we designed agents **4**–**6**, **8**, and **9** with side chains at the 2- or 4-position of the acridine ring (**4**–**6**) or attached to the triaminotriazine rings (**8** and **9**).

DOI: 10.1021/jacs.5b09266
J. Am. Chem. Soc. 2015, 137, 14180–14189

Chart 1

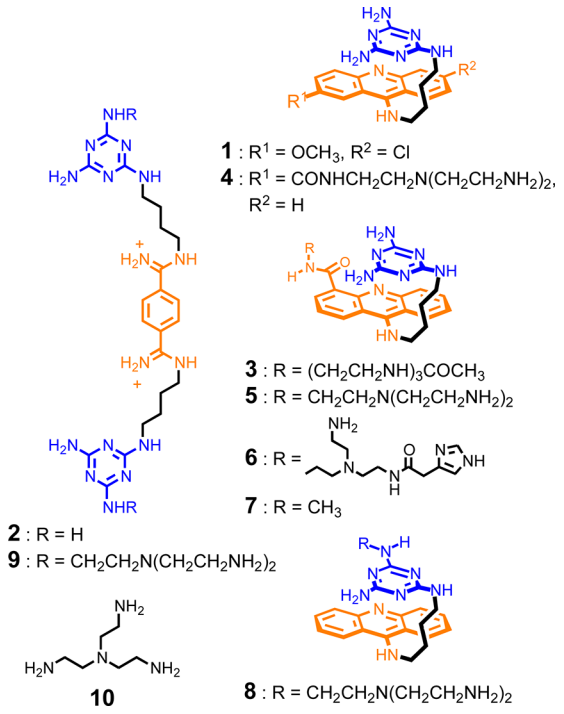

The ability of these potentially catalytic functional groups to perform in the desired fashion was examined by modeling. Thus, the ligands were docked to binding sites prepared from the published X-ray analysis of $(CUG)_6$ (PDB: 3GM7) using MOE (Figure S1), and each was found to reach at least one putative scissile phosphate bond. The synthesis of cleaving agents **4**–**6**, **8**, and **9** is straightforward (Schemes S1–S4) and generally involved conjugation of di-Boc-protected tris(2-aminoethyl)amine with the appropriate acridine acid chloride or chlorotriazine. The imidazole-bearing agent **6** was prepared from **5** by coupling one amino group with imidazole-4-acetic acid. The additional functional groups improved the water solubility, cell penetration, and affinity toward CUG^{exp} (vide infra and Figure S2).

DNA-Targeted Activity. Inhibition of $(CTG{\cdot}CAG)_{74}$ Transcription by 5, 6, and 9 *in Vitro*. As described above, simple ligand **1** binds CTG sites tightly, whereas **2** does not. Nonetheless, the additional ammonium groups in **9** might potentially increase its affinity for both CTG DNA and CUG RNA, so we examined its potential for inhibition of CTG^{exp} transcription along with that of ligands **5** and **6**. The *in vitro* $(CTG{\cdot}CAG)_{74}$ transcription assays utilized a T7 promoter located in the upstream region of the repeats.[32] Ligands **5** and **9** strongly inhibited the production of CUG^{exp} and in a dose-dependent manner, whereas ligand **6** showed less inhibition. Control ligands **2**, **7**, and **10** had negligible effects on the transcription of $(CTG{\cdot}CAG)_{74}$ (Figure 2 and Figure S3).

To test the selectivity and potentially the target of the inhibition, we performed similar experiments with two separate control plasmids each lacking repeats (see Experimental Section for details). Ligand **6** showed negligible transcription inhibition at all tested concentrations, which ranged from 1 to 100 μM, whereas **9** strongly inhibited the transcription of the control plasmids at higher concentrations (i.e., 50 and 100 μM) (Figure S3). However, **9** did show some selectivity in the inhibition with only 30% inhibition of the control plasmids observed at 10

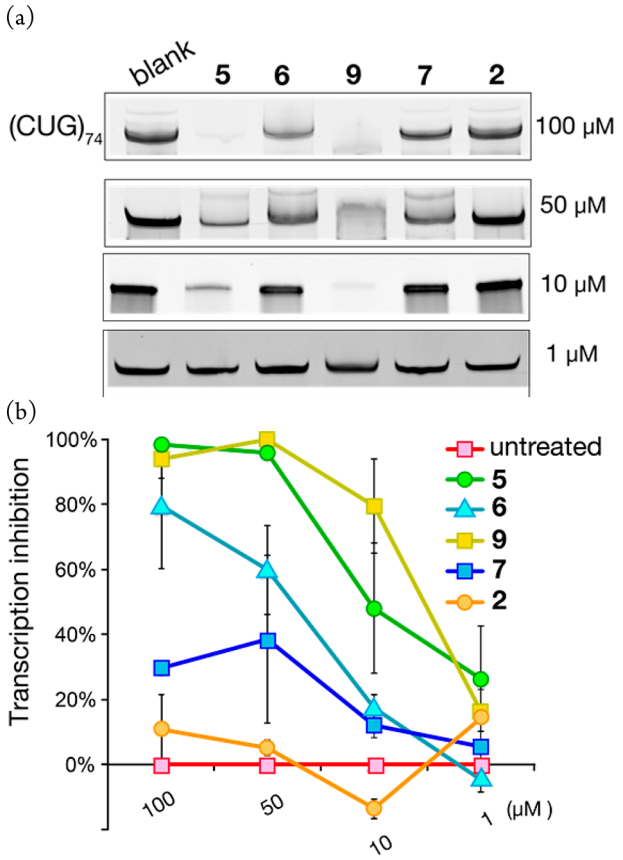

Figure 2. *In vitro* transcription of $(CTG{\cdot}CAG)_{74}$. Ligands at different concentrations were incubated with 15 ng of linearized plasmids in T7 RNA polymerase mixture at 37 °C. After 2 h, the reaction mixture was loaded on a 8% denaturing gel. (a) Transcription gels of ligands at different concentrations. (b) Plot of the percentage of transcription inhibition versus ligand concentrations. The error bars represent standard errors of mean of three independent experiments.

μM, whereas ca. 80% inhibition was obtained for the plasmid containing $(CTG{\cdot}CAG)_{74}$ (Figure 2b).

The lack of binding affinity shown by **2** toward $d(CTG)_{12}$, $d(CAG)_{12}$, and $d(CTG{\cdot}CAG)_{12}$ (Table 1 and Figure S4a),

Table 1. Equilibrium Dissociation Constants (apparent K_D, μM) of Ligands 2 and 9 to Various Oligonucleotides Determined by ITC[a]

hairpin/duplex	2	9
$(CUG)_{12}$	8 ± 2[b]	6 ± 4
$d(CTG)_{12}$	nb	5 ± 1
$d(CAG)_{12}$	nb	nb
$d(CTG{\cdot}CAG)_{12}$	nb	nb

[a]Apparent K_D values were determined from at least three independent experiments; nb indicates no detectable binding. [b]Data from Wong (ref 12).

combined with the transcription inhibition data collected for **9**, supports the notion that the added ammonium groups do indeed increase its affinity for CTG^{exp}. To directly assess the DNA-targeting ability of **9**, ITC experiments were performed with oligonucleotide analogues of the various trinucleotide repeat sequences (Table 1 and Figure S4b). In contrast to **2**, **9** showed comparable binding affinities toward $d(CTG)_{12}$ and $(CUG)_{12}$ hairpin structures. This supports the idea that **9**

DOI: 10.1021/jacs.5b09266
J. Am. Chem. Soc. 2015, 137, 14180–14189

inhibits the transcription of CTG^{exp} by stabilizing its hairpin structure. Indeed, no strong binding was detected for $d(CAG)_{12}$ or $d(CTG{\cdot}CAG)_{12}$ (Table 1 and Figure S4b). The *in vitro* transcription experiments using $(CTG{\cdot}CAG)_{74}$ and compounds **2**, **5**–**7**, and **9** were repeated but with $(CUG)_{16}$ added as a competitor. In each case, the transcription inhibition of ligands was reduced, particularly for **6** (Figure S5).

RNA-Targeted Activity. *In Vitro* CUG^{exp} Cleavage by Small Molecules 4–9. The potential cleavage activity of **4**–**9** was screened using a simple gel shift assay with $(CUG)_{16}$. Thus, each agent was incubated for 18 h with unlabeled $(CUG)_{16}$ at a final concentration of 100 μM at pH 7.4. The mixture was separated on an RNA denaturing gel and stained with EtBr (Figure 3). No loss of $(CUG)_{16}$ intensity was observed upon

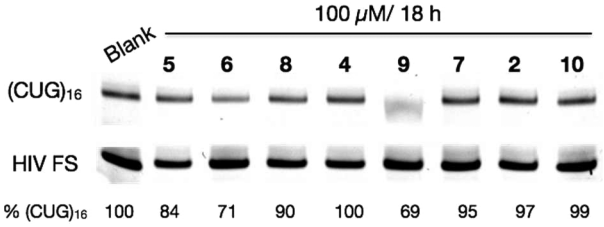

Figure 3. Cleavage screening gel. $(CUG)_{16}$ (100 nM) was incubated with ligands (100 μM) in a Tris buffer (pH 7.4) containing 150 mM NaCl and 2 mM $MgCl_2$, 18 h, 37 °C. HIV FS RNA (1 pmol) was used as an internal standard. The reaction mixture was loaded onto a 20% denaturing PAGE gel, and RNA was detected by poststaining with EtBr. Normalized % $(CUG)_{16}$ intensity was reported as the average value of two independent experiments.

treatment with **2**, **7**, or tris(2-aminoethyl)amine (**10**), demonstrating that a polyamine or the CUG-targeting acridine or bisamidinium ligand on its own is insufficient to alter the $(CUG)_{16}$. In contrast, a decrease in $(CUG)_{16}$ intensity was observed for ligand **5**, **6**, **8**, and **9**, each containing amino groups, providing evidence of RNA cleavage (Figure 3). At least qualitatively, agents **6** and **9** appeared to be most active.

To observe potential cleavage fragments that were not observable in the screening gel due to the relative insensitivity of the EtBr poststaining, we performed similar experiments using 5′-TAMRA-labeled $(CUG)_{16}$ (T-$(CUG)_{16}$). As seen in Figure 4 and Figure S6a, after 60 h of incubation, agent **9** shows a large number of bands. Interestingly, the intensity pattern corresponds to the repeat sequence, with every fourth band significantly more intense. This pattern may indicate a specific positioning of the catalytic groups by the ligand or possibly a higher reactivity of the UU mismatch site. Similar, although less distinct, patterns were seen at shorter (20 h) incubation times (see Figure S6b, which includes data for **6** and **9**). RNA fragments were observed for a control incubation using a combination of ligand **2** and tetraamine **10**, but the reaction was much slower (Figure S6a, labeled C). Given the simplicity and ease of quantifying the loss of unlabeled $(CUG)_{16}$ in the screening assay above, agent **9** was re-examined at four different concentrations (5–100 μM) and three times. As seen in Figure 5 and Figure S6c, loss of the $(CUG)_{16}$ band was both time- and dose-dependent.

To better determine the origin of the loss of CUG^{exp} mRNA, the reaction of $(CUG)_4$ with a 3′-TEG-biotin tag and **6** was monitored by MALDI. After 5 h of incubation with **6**, fragment peaks were observed with lower m/z values, but no major change was seen in control samples (Figure S7). The m/z

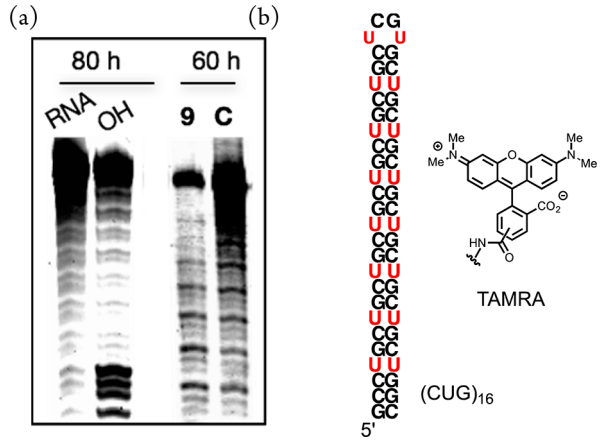

Figure 4. (a) Partial TAMRA–$(CUG)_{16}$ cleavage gel. Ligand **9** or a control C as mixture of **2** (100 μM) and **10** (100 μM) was incubated with T-$(CUG)_{16}$ (100 nM) in a Tris buffer (50 mM, pH 7.4) supplemented with 150 mM NaCl and 2 mM $MgCl_2$. OH is a control with RNA incubated in a buffer at pH 10.6. The reaction mixture was run on a 20% denaturing PAGE gel. See Figure S6a for full gel. (b) $(CUG)_{16}$ and TAMRA structures.

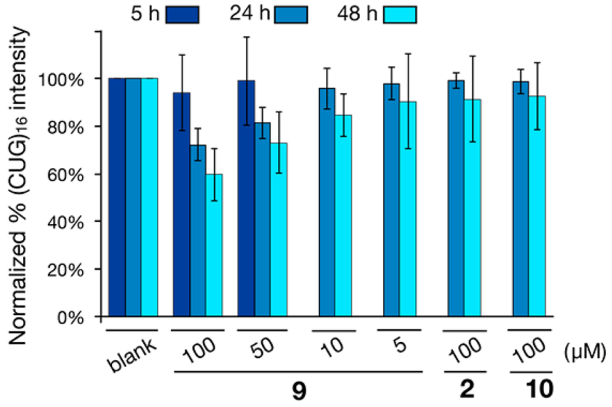

Figure 5. Time- and dose-dependent cleavage experiments of ligand **9** using $(CUG)_{16}$. Quantitative analysis of changes in $(CUG)_{16}$ intensity. The reaction mixture was loaded on a 20% denaturing PAGE gel. The percentage of $(CUG)_{16}$ intensity was normalized to the control (no compound). Error bars represent standard errors of mean of three independent experiments.

values found matched the calculated m/z corresponding to hydrolysis products with 3′-hydroxyl end groups and selective cleavage in the loop and immediately adjacent to the loop. Cleavage experiments at different pH values and different concentrations of Mg^{2+} were carried out. The data from these experiments showed that the cleavage activity of ligand **9** was Mg^{2+}-independent and increased with increasing pH (Figure S8). The higher pH increases the concentration of the anticipated active species containing one amino group and one ammonium ion; however, the higher pH also increases the background hydroxide-catalyzed reaction.

Selectivity of CUG^{exp} Cleaving Agents. Off-target activity is a concern for any therapeutic agent but especially one designed to chemically alter its target (e.g., cleave RNA). To test the selectivity of agents **6** and **9**, the cleaving gel assay described above was applied to other RNA targets, specifically cTNT32, $(CCUG)_8$, and HIV-1 frameshift site RNA (HIV FS) (Figure 6). Both **6** and **9** were quite selective. Thus, neither agent showed detectable cleavage of cTNT32 or HIV FS,

DOI: 10.1021/jacs.5b09266
J. Am. Chem. Soc. 2015, 137, 14180–14189

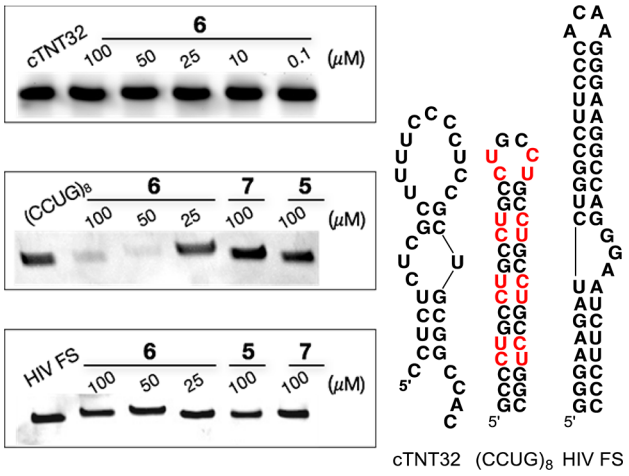

Figure 6. Selectivity study. Structures of RNA oligonucleotides tested in the selectivity study. Gels of potential cleavage of alternative RNA targets by ligand **6**. RNA (100 nM) was incubated with ligands for 19 h at 37 °C. The reaction mixture was loaded on a 20% denaturing PAGE gel, followed by poststaining with EtBr. For ligand **9**, see Figure S9a.

despite both of these RNAs having structures loosely analogous to CUG^{exp} (Figure 6 and Figure 9a). Both similarly adopt stem-loop structures with internal loops within the stem, although obviously of different sequence. Differences between **6** and **9** were observed with the former cleaving $(CCUG)_8$, the toxic RNA involved in myotonic dystrophy type 2 (DM2) (Figure 6 and Figure S9b). In contrast, **9** showed no activity toward $(CCUG)_8$. The ability to process the RNA directly parallels the corresponding ligand−RNA binding affinities. Thus, **1**, which contains the acridine−triazine core of agent **6**, complexes $(CCUG)_6$[33] and $(CUG)_n$ sequences (see also Figure S2). Likewise, **2** (the core of agent **9**) complexes $(CUG)_n$ but showed no affinity toward $(CCUG)_8$, cTNT32, or HIV FS.[12] These data are consistent with the catalytic functionality being brought into proximity of the RNA through selective binding.

Bioactivity of Agents 5, 6, and 9 in DM1 Model Cells. The ability of **5**, **6**, and **9** to disrupt the MBNL1−CUG^{exp} interaction in cells was evaluated using model DM1 cells. Thus, HeLa cells were transfected with GFP-DT0 or GFP-DT960 plasmids that contain 0 or 960 interrupted CTG repeats, respectively, in exon 15 of a truncated *DMPK* gene.[19,22] The plasmids express both GFP protein and CUG^{exp} under the activation of doxycycline (Dox), with GFP being used as a marker for successful transfection and expression of the plasmids in the cells. Treatment of the DM1 model cells with ligands at 50 μM for 48 h was followed by analysis using confocal microscopy. As seen in the representative images in Figure 7, each of the three agents inhibited nuclear foci formation, leading to the dispersion of MBNL1 protein throughout the nucleus (see Figure S10 for images of more cells).

Because **9** is less toxic to HeLa cells than **5** and **6**, it was selected for a splicing study of insulin receptor (*IR*) minigene. Splicing of *IR* minigene is misregulated with the abnormal exclusion of exon 11 because of the MBNL1 depletion in DM1 cells.[34] DM1 model cells, in this case HeLa cells cotransfected with plasmids containing *IR* minigene and $(CTG)_{960}$, were treated with **9** at 100 μM for 3 days, leading to a 77% rescue of the *IR* splicing defect (Figure S11).

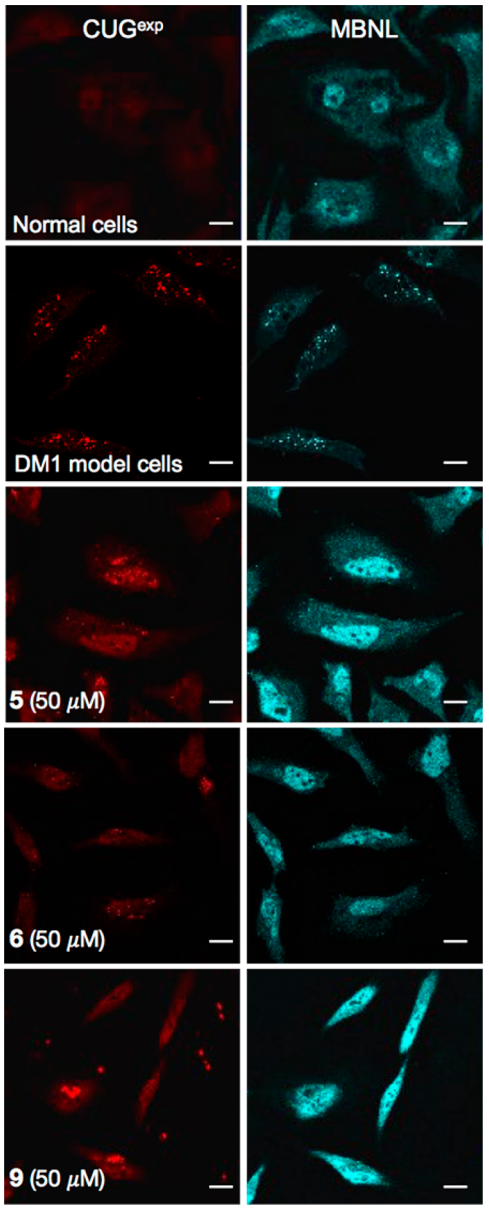

Figure 7. Foci dispersion by agents **5**, **6**, and **9**. DM1 model cells were incubated with 50 μM ligand for 48 h. Cells were fixed, and CUG^{exp} was stained with Cy3-$(CAG)_{10}$, and MBNL1 was probed with mouse anti-MBNL followed by staining with goat anti-mouse Alexa 647 secondary antibody. The scale bar is 10 μm.

Encouraged by the promising results from the *in vitro* cleavage and the ability of **5**, **6**, and **9** to enter cells and dissolve MBNL1−CUG nuclear foci, we performed experiments to study whether the agents could control the level of toxic CUG^{exp} in cells using a reported protocol.[19,22] Two sets of cells, transfected with either GFP-DT0 or GFP-DT960 plasmids, were incubated with **5**, **6**, or **9** for 3 days. The CUG^{exp} mRNA level was determined by measuring the level of exon 15 upstream of the CUG^{exp} relative to *PABP* mRNA as a control, followed by normalizing the values to the levels measured from untreated cells. As seen in Figure 8a, there was a 60−70% reduction in CUG^{exp} levels in cells treated with **6** and **9** at 50 μM. Ligand **5** showed only a negligible change of CUG^{exp} levels, although a longer incubation time of 5 and 7 days led to a significant decrease in the level of toxic CUG^{exp} RNA (Figure

DOI: 10.1021/jacs.5b09266
J. Am. Chem. Soc. 2015, 137, 14180−14189

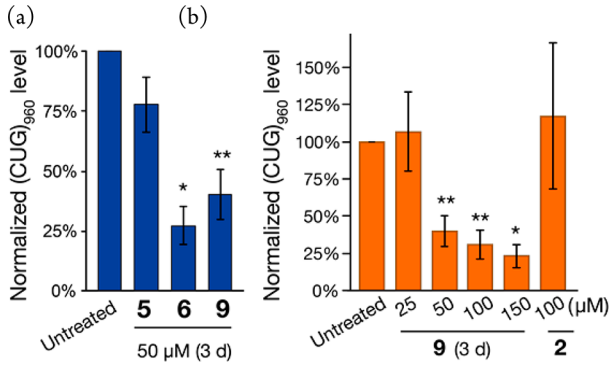

Figure 8. CUG^{exp} mRNA levels in DM1 model cells. (a) Effects of ligands **5**, **6**, and **9** on CUG^{exp} mRNA levels at 50 μM for 3 day treatment. (b) Ligand **9** reduced CUG^{exp} mRNA levels in a dose-dependent fashion. Error bars represent the standard error of mean of at least three independent experiments; *P < 0.01, **P < 0.005 (two-tailed t-test).

S12a). Because of its lower toxicity, the dose dependence of **9** was examined by treating cells with four different concentrations ranging from 25 to 150 μM. As seen in Figure 8b, **9** clearly regulates the cellular CUG^{exp} mRNA levels in a dose-dependent manner. The control ligands **2** and **3** did not show a significant effect on the levels of toxic RNA (Figure 8b and Figure S12b).

Ligand 9 Suppresses Neurodegeneration, Regulates CUG^{exp} mRNA Levels, and Improves Both the Rough Eye Phenotype and Larval-Crawling Defect in DM1 *Drosophila*. The data presented above indicate that **9** is able to engage each of three small-molecule intervention pathways outlined in Figure 1b, and it was found further to be relatively nontoxic. For these reasons, it was selected for *in vivo* testing in a DM1 *Drosophila* model,[12] specifically transgenic flies that express an interrupted $(CTG)_{480}$ sequence ($i(CTG)_{480}$). The flies exhibit severe neurodegeneration and manifest a number of disease symptoms, including the well-characterized glossy and rough-eye phenotype that can be easily observed microscopically (Figure 9a). Treatment of the DM1 flies with ligand **9** improved the neurodegenerative phenotype in a dose-dependent fashion. Particularly striking is a significant reduction in glossiness and a better-defined eye shape clearly observed after a 6 day treatment regimen (Figure 9a and Figure S13). As we previously reported, control ligand **2** also showed reversal of the disease phenotype but less effectively.

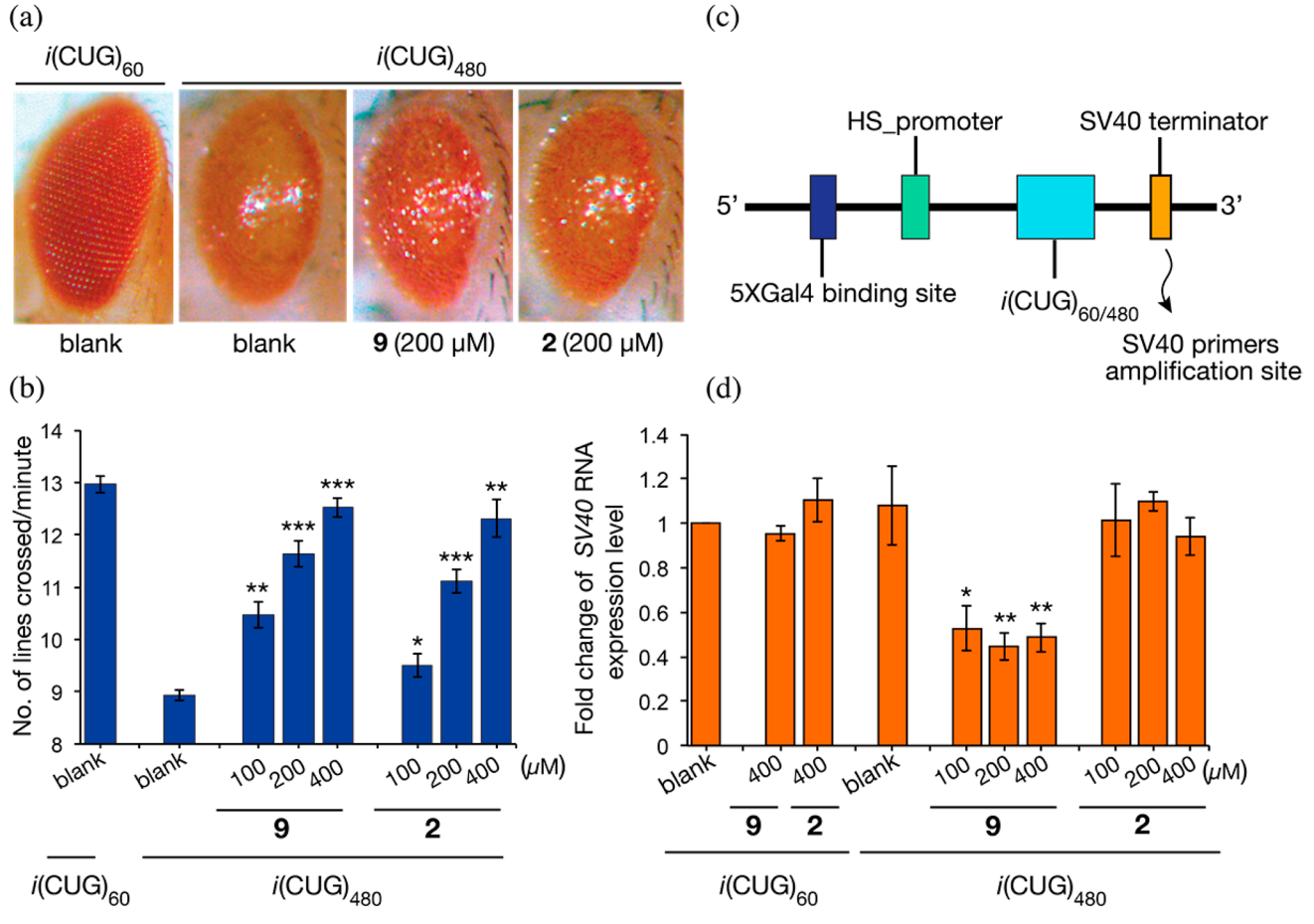

Figure 9. Biological activities of ligands in DM1 *Drosophila*. (a) Ligands **2** and **9** improved the neurodegeneration in DM1 *Drosophila* at 6 days age; **9** showed better effects than **2** under the same conditions. (b) Larvae mobility was improved after the treatment of ligands. The error bars represent standard deviation of three independent experiments. For each independent experiment, 10 individual larvae were studied. (c) Diagram of $i(CTG)_{60/480}$ gene construct and the region (*SV40* terminator) that was amplified to measure the level of transcribed mRNA. (d) Ligand **9** reduced the levels of *SV40* RNA in larvae. The *SV40* region of the *CUG*-containing RNA was measured relative to β-actin RNA level. The error bars represent the standard deviation of three independent experiments. For each independent experiment, mRNA levels from five individual larvae were determined; *P < 0.05, **P < 0.01, ***P < 0.001 (two-tailed t-test).

DOI: 10.1021/jacs.5b09266
J. Am. Chem. Soc. 2015, 137, 14180−14189

These DM1 *Drosophila* exhibit other phenotypes, including impaired locomotion. To test the ability of **2** and **9** to improve the locomotor behavior of *Drosophila* larvae, we used crawling assays.[35−37] Untreated larvae having $i(CUG)_{60}$ do not show the phenotype and crawled with an average speed of ca. 13 lines/min, which is considered baseline locomotion. Those expressing $i(CUG)_{480}$ crossed only 9 lines/min (Figure 9b; see supporting movie). Larvae that were treated with the highest doses of **2** and **9** (400 μM) showed significant improvement in locomotion with an average crawling speed approaching the normal baseline level of ca. 13 lines/min. Importantly, the phenotypic improvement with both compounds was dose-dependent, and **9**, in all cases, provided greater phenotypic reversal than did **2**. Thus, with doses ranging from 100 to 400 μM, **9** exhibited between 38 and 89% recovery of normal locomotor behavior, whereas **2** showed between 14 and 83% recovery (Figure 9b).

Because **9** regulated the level of toxic CUG^{exp} in cells, we performed experiments to determine whether the same activity was observed in DM1 flies. *SV40* terminator mRNA is downstream from the $i(CUG)_{60}$ and $i(CUG)_{480}$ regions (Figure 9c). Thus, its amplification using specific primers that are detailed in the Experimental Section is directly correlated with CUG^{exp} mRNA levels. The *SV40* mRNA was expressed approximately equally in larvae bearing either $i(CUG)_{60}$ or $i(CUG)_{480}$ (Figure 9d). Treatment with **2** and **9** at 400 μM showed no change in *SV40* mRNA levels measured in larvae having $i(CUG)_{60}$. In contrast and consistent with the cell studies, **9** reduced by ca. 40−60% the *SV40* mRNA levels in the $i(CUG)_{480}$ larvae, whereas **2** did not. This result demonstrates the *in vivo* selectivity of **9** toward larvae expressing disease-length CUG trinucleotide repeats.

CONCLUSION

The "holy grail" of DM1 therapeutic strategies would involve contraction of CTG^{exp} to nondisease lengths. Such a process could represent a cure for the disease. This is a particularly difficult challenge because multiple processes cause the expansion and their detailed mechanisms are not known. For this reason, drug discovery efforts to date have largely focused on the toxic CUG^{exp} transcript and its gain-of-function mechanism. A number of single-target small molecules are now known that selectively recognize CUG^{exp} and liberate sequestered MBNL1. However, recent reports indicate a more complex disease pathobiology, suggesting that binding CUG^{exp} may not be enough to reverse all disease pathways. Thus, efforts to destroy the toxic RNA transcript or inhibit its formation have particular appeal. Three reported examples of agents that control CUG^{exp} levels include antisense agents that induced CUG^{exp} cleavage via a RNase H-dependent manner,[22] a small molecule that degraded CUG^{exp} through a photo-induced cleavage,[24] and $(CTG{\cdot}CAG)_n$ transcription inhibitors.[25]

The efforts described herein sought a single small-molecule agent that might intervene in multiple DM1 disease pathways. We discovered agents **5**, **6**, and **9** that, indeed, operate in three distinct ways. Each shows RNase-A-like activity in selectively cleaving $(CUG)_{16}$ *in vitro*, and each inhibits both the *in vitro* transcription of CTG^{exp} and the sequestration of MBNL1 into nuclear foci in a DM1 model cell culture. Not all of the compounds performed equally well at each of these tasks. For example, **6** and **9** cleaved $(CUG)_{16}$ more rapidly than did **5**, and both fully inhibited nuclear foci formation, whereas **5** was not quite as effective. As a CTG^{exp} transcription inhibitor, **9** was the most effective but less selective than **6**. Interestingly, the least effective transcription inhibitor, **6**, was most effective at suppressing cellular levels of $(CUG)_{960}$. Although this might suggest that the RNA cleaving activity is most important, the cellular suppression of $(CUG)_{960}$ over the 3 day period appears to well out-pace the *in vitro* RNA cleavage rates. The latter are quite slow even at high compound concentrations. It is possible that one or more RNA nicks activate an endogenous RNase, or it may just reflect the complexity of the cell where $(CUG)_{960}$ suppression will depend on many factors, including cell permeability and the effectiveness of the three separate targeting activities in the complex environment of the cell.

With all of the results and particularly the low cytotoxicity exhibited by **9** taken into account, it was considered the most promising candidate for *in vivo* studies. In a DM1 *Drosophila* model, **9** was found to rescue the neurodegeneration, thereby significantly reversing both the rough-eye phenotype and the larvae locomotor function. How does **9** function in the *Drosophila*? To the best of our knowledge, **9** is the first small molecule to control the level of CUG^{exp} in a DM1 model organism. It is beyond the scope of this investigation to determine how **9** functions *in vivo*, but the reduction in the toxic RNA levels supports the role of its multi-target ability observed in earlier studies. It was especially noteworthy that control compound **2** shows no suppression of the CUG^{exp} levels.

None of the compounds described herein are able to recognize or affect the $(CAG)^{exp}$ transcript, so it is able to undergo RAN translation. It is also the case that agents such as **5**, **6**, and **9** that nick RNA and may act as transcription inhibitors will have to exhibit a very high level of selectivity to avoid undesirable off-target activity. Indeed, in the transcription assays with **9**, some inhibition was observed with the control sequences. Although achieving such selectivity remains as a future challenge, the repeating nature of the trinucleotide repeat target means that a bi- or polyvalent strategy can easily amplify selective targeting. Most significantly, we have demonstrated the first rational multi-target drug discovery effort that has led to three small molecules that intervene in three separate pathobiological steps in DM1, with one of the agents showing enhanced phenotypic reversal in two separate DM1 *Drosophila* assays.

EXPERIMENTAL SECTION

Compounds, Materials, and General Methods. The preparation and characterization of ligands tested in the cellular experiments are reported herein. Other synthetic procedures can be found in detail in the Supporting Information. Unless otherwise noted, ^{1}H spectra were recorded on a 500 MHz Varian Unity Inova spectrometer. All NMR measurements were carried out at ambient temperature. Chemical shifts are in parts per million (ppm). Coupling constants (J) are reported in hertz (Hz). Electrospray ionization mass spectra (ESI-MS) were obtained by the Mass Spectrometry Laboratory, School of Chemical Sciences, University of Illinois at Urbana—Champaign. All tested ligands are ≥95% pure as indicated by HPLC.

Ligand 5. To a 50 mL round-bottomed flask containing 280 mg (0.5 mmol) of di-*tert*-butyl (((2-(9-chloroacridine-4-carboxamido)-ethyl)azanediyl)bis(ethane-2,1-diyl))dicarbamate in 20 mL of anhydrous DMF were added 109 mg (0.6 mmol) of N^2-(4-aminobutyl)-1,3,5-triazine-2,4,6-triamine and 0.19 mL (1.1 mmol) of DIPEA. The reaction was stirred at 60 °C for 6 h. DMF was removed under high vacuum, affording an orange solid. The crude solid was dissolved in 5 mL of dichloromethane and purified by alumina (activated, basic)

DOI: 10.1021/jacs.5b09266
J. Am. Chem. Soc. 2015, 137, 14180−14189

column chromatography using 95:5 (v/v) DCM/MeOH as eluent, giving 240 mg (67%) of the desired compound as an orange solid.

To a 100 mL round-bottomed flask containing 240 mg (0.4 mmol) of the orange solid in 40 mL of dichloromethane was added 10 mL (131 mmol) of trifluoroacetic acid. The reaction was stirred at room temperature for 6 h. The solvent was removed using a rotary evaporator and dried under vacuum to give 410 mg (100%) of compound **5** as a yellow solid, TFA salt: ^{1}H NMR (D_2O) δ 8.40 (br d, Ar*H*, 1H, J = 8.5), 8.22 (br d, Ar*H*, 1H, J = 8.5), 8.12 (dd, Ar*H*, 1H, J = 1.5, 6), 7.81 (td, Ar*H*, 1H, J = 1.5, 7.5), 7.66 (d, Ar*H*, 1H, J = 7.5), 7.41 (br t, Ar*H*, 2H, J = 8.3), 4.05 (br t, CH_2, 2H, J = 6.5), 3.55 (t, CH_2, 2H, J = 7), 3.15 (br t, CH_2, 2H, J = 6.3), 3.10 (br t, CH_2, 4H, J = 6.5), 2.99 (br t, CH_2, 4H, J = 6.5), 2.93 (br t, CH_2, 2H, J = 7), 1.85 (br q, CH_2, 2H, J = 7), 1.58 (br q, CH_2, 2H, J = 7); ESI-MS (m/z) calcd for $[M + H]^+$ 547.3; found 547.3 $[M + H]^+$.

Ligand 6. To a 20 mL round-bottomed flask containing 200 mg (0.4 mmol) of compound **5** in 5 mL of DMF was added Et_3N to pH 7. The mixture of 101 mg (0.6 mmol) of 4-imidazole acetic acid and 129 mg (0.6 mmol) of DCC in 5 mL of DMF was added to the above solution. The reaction was stirred at room temperature overnight. The solvent was removed under vacuum. The crude product was purified using a reversed-phase C18 column on a CombiFlash system (MeOH/H_2O (v/v) = 0:100 to 50:50) to afford 15 mg (12%) of compound **6** as a yellow solid (15 mg, 12%): ^{1}H NMR (D_2O) δ 8.56−8.50 (m, Ar*H*, 1H), 8.48 (br s, Ar*H*, 1H), 8.39−8.31 (m, Ar*H*, 1H,), 8.25 (br d, Ar*H*, 1H, J = 8), 7.94 (br t, Ar*H*, 1H, J = 8), 7.78 (br t, Ar*H*, 1H, J = 8.5), 7.54 (br t, Ar*H*, 2H, J = 8), 7.12 (s, C*H*, 1H), 4.19 (br t, CH_2, 2H, J = 6.8), 3.68 (br s, CH_2, 2H), 3.46 (br t, CH_2, 2H, J = 6.5), 3.30−3.21 (m, CH_2, 4H), 3.18−3.09 (m, CH_2, 4H), 3.02−2.96 (m, CH_2, 2H), 2.96−2.91 (m, CH_2, 2H), 2.03−1.96 (m, CH_2, 2H), 1.74−1.69 (m, CH_2, 2H); ESI-MS (m/z) calcd for $[M + H]^+$ 655.4; found 655.8 $[M + H]^+$, 328.5 $[M + 2H]^{2+}$.

Ligand 9. To a 100 mL oven-dried round-bottomed flask was added 250 mg (0.9 mmol) of diethyl terephthalimidate hydrochloride. The white solid was dissolved in 15 mL of anhydrous ethanol. To the resulting suspension was added 0.3 mL (2.2 mmol) of anhydrous Et_3N followed by 1.0 g (1.9 mmol) of di-*tert*-butyl (((2-((4-amino-6-((4-aminobutyl)amino)-1,3,5-triazin-2-yl)amino)ethyl)azanediyl)bis-(ethane-2,1-diyl))dicarbamate at once. The resulting suspension was stirred at room temperature for 1 day. The solvent was removed using a rotary evaporator. The crude was dissolved in 20 mL of 2 N ethanolic HCl. The reaction was stirred at room temperature overnight. Ethanol was removed using a rotary evaporator. The crude was purified by a Sephadex CM-25 column chromatography using an aqueous solution of NH_4HCO_3 from 0.1 to 1.0 M. Fractions containing products were combined and concentrated at 60 °C using a rotary evaporator. The solid was dissolved in 80 mL of 0.1 M aqueous HCl. The resulting solution was concentrated using a rotary evaporator to give 390 mg (40%) of compound **9** as a white HCl salt: ^{1}H NMR (DMSO-d_6) δ 10.27 (br s, N*H*, 2H), 9.80 (br s, N*H*, 2H), 9.46−9.41 (m, N*H*, 2H), 8.42−7.90 (m, Ar*H*, 8H), 8.00 (s, Ar*H*, 4H), 3.87 (br s, NH_2, 8H), 3.54−3.35 (m, CH_2, 12H), 2.96 (br s, CH_2, 8H), 2.76−2.62 (m, CH_2, 12H), 1.71−1.64 (m, CH_2, 8H); ESI-MS (m/z) calcd for $[M + H]^+$: 781.6; found 781.6.

RNA was purchased from Integrated DNA Technologies (Coralville, IA) and GE Dharmacon (Lafayette, CO). RNA samples were dissolved in THE Ambion RNA storage solution and stored at −20 °C. UV absorbance of the RNA solutions was measured at 25 °C on a Shimadzu UV-2501PC spectrophotometer. The concentration of the double-stranded RNA was calculated using Beer's law with the extinction coefficient at 260 nm provided by the supplier.

RNA Cleavage Experiments. RNA was fast-folded at 95 °C for 5 min and then placed in ice for 10 min. RNA with a final concentration of 100 nM was incubated with 100 μM cleaving agents (in screening assays) or with ligand **9** at different concentrations (5, 10, 50, 100 μM). The cleaving buffer was 50 mM Tris buffer (pH 7.4) containing 150 mM NaCl and 2 mM $MgCl_2$. The final volume of the reaction mixture was 10 μL. The reaction was quenched by adding 8 μL of 8 M urea and 2 μL of RNA loading dye or 1 μL of HIV FS RNA as a spike and 1 μL RNA loading dye (in screening experiments) followed by heating at 95 °C for 5 min. The reaction mixture was separated on a 20% RNA denaturing gel. For nonlabeled RNA, the gel was stained with EtBr and observed under UV. For TAMRA−$(CUG)_{16}$, the gel was scanned using a Typhoon instrument in the Biotech Center Lab (Noyes Laboratory, School of Chemical Sciences, University of Illinois, Urbana, IL). The images were worked up using ImageJ software (NIH).

Foci dispersion and *IR* splicing experiments followed the reported protocols.[12] The details of experiments can be found in the Supporting Information.

Cellular mRNA Level Study with Dox Treatment. Approximately, 50 000 HeLa cells were plated on a 12-well plate in DMEM media supplemented with high glucose, L-glutamine, and no antibiotics a day before transfection. HeLa cells were transfected with 1 μg of GFP-DT0 or GFP-DT960 plasmids using Lipofectamine (Life Technologies) following the recommended protocol. After 4 h, the transfection cocktail was replaced with the growing media, and cells were treated with 1 μg of Dox. Ligands were treated at the same time at desired concentrations for 3 days. Cells were checked under fluorescence microscopy for a GFP signal as a marker of successful transfection and then harvested. Total mRNA was isolated using E.Z.N.A. total RNA kit I (Omega). Approximately, 1.5 μg of total mRNA was subjected to DNase treatment to remove all DNA contaminant. cDNA synthesized using Iscript cDNA synthesis kit (Bio-Rad) was used as the template for real-time PCR using SYBR master mix (Applied Biosystem). The results from real-time PCR experiments were analyzed using the $\Delta\Delta C_t$ method.[38] The mRNA levels of exon 15 upstream of CUG^{exp} were measured relative to *PABP* mRNA levels. The difference in the expression level of exon 15 RNA transcript between treated GFP-DT0 and GFP-DT960 samples was compared with the one of untreated samples that were normalized to 100%. The primers were used in the experiments: E15upF: 5′-TCG GAG CGG TTG TGA ACT-3′; E15upR: 5′-GTT CGC CGT TGT TCT GTC-3′; PabpF: 5′-CTG CTG TTC ATG TGC AAG GT-3′; PabpR: 5′-CAA CAG CAT GCC AGT GAT T-3′.

***In Vitro* Transcription of $(CTG{\cdot}CAG)_{74}$.** A 10 μL mixture contained 15 ng of linearized plasmid $(CTG)_{74}$ or control plasmid templates, 0.5 mM each rATP, rCTP, rGTP, and rUTP, and 0.5 U T7 polymerase (Biolab) in 1× T7 transcription buffer (80 mM Tris pH 8.3, 10 mM $MgCl_2$, 2 mM spermine, 0.1% Triton-X, 10 mM NaCl) was incubated at 37 °C for 2 h. Ligand was added with the final concentrations of 0, 1, 10, 50, and 100 μM prior to incubation. Reactions were quenched by adding 8 μL of 8 M urea and 2 μL of denaturing dye (95% formamide, 5 mM EDTA, 0.025% each xylene cyanol and bromophenol blue) and heating to 95 °C for 5 min. Of this solution, 15 μL was run on a 8% denaturing polyacrylamide gel in 0.5× TBE. The gel was stained with EtBr. Bands were quantified using the ImageJ (NIH). The intensity of $(CUG)_{74}$ band (ca. 260 nt) was normalized to that from the untreated transcription reaction. The control plasmids were *pTRI-Xef* plasmid provided with MEGAscript T7 transcription kit (Life Technologies) that expresses 1.89 kb RNA transcript and another non-repeat-containing plasmid expressing a 197 nt RNA transcript.

Drug Treatment in *Drosophila*. *Drosophila* lines were cultured in standard cornmeal medium supplemented with dry yeasts. Fly lines bearing *UAS-*$(CTG)_{60}$ and *UAS-*$(CTG)_{480}$[39,40] were kind gifts of Prof. Rubén Artero Allepuz (Universitat de València, Estudi General, Spain). The *gmr-GAL4*[41] and *24B-GAL4*[42] lines were used to drive *UAS* transgene expression in eye and muscles, respectively. Ligands **2** and **9** were dissolved in ddH_2O and mixed with fly food. Genetic crosses were set up in drug-containing fly food at 21.5 °C for external eye assay and at 25 °C for larval crawling assay and real-time PCR analysis. For additional details, see ref 12.

Larval Crawling Assay. Larval crawling assays were performed as described in Lanson et al.[35] Ten wandering third instar larvae were washed in ddH_2O and placed on a 2% agarose gel in a 15 cm Petri dish with gridlines spaced at 0.5 cm. The larvae were allowed to acclimate for a period of 1 min, and the total number of gridlines that the posterior end of the larvae passed in 1 min was determined. Each set of

DOI: 10.1021/jacs.5b09266
J. Am. Chem. Soc. 2015, 137, 14180−14189

experiments was repeated independently three times using larvae collected from separate genetic crosses.

RNA Extraction and Real-Time PCR. RNA was extracted from third instar larvae by TRIzol reagent (Invitrogen). One microgram of purified RNA was used for reverse transcription via the ImPromII reverse transcription system (Promega). Real-time PCR gene expression assays were performed on an ABI 7500 real-time PCR system, using the SYBR Green PCR master mix (ABI) with the following primers: *SV40*_F: 5′-GGA AAG TCC TTG GGG TCT TC-3′; *SV40*_R: 5′-GGA ACT GAT GAA TGG GAG CA-3′; *actin*_F: 5′-ATG TGC AAG GCC GGT TTC GC-3′ and *actin*_R: 5′-CGA CAC GCA GCT CAT TGT AG-3′. Each reaction was performed in duplicate. Quantification of gene expression was calculated according to the $2^{-\Delta\Delta C_t}$ method, where $\Delta\Delta C_t = (C_{t,target} - C_{t,actin})_{experimental} - (C_{t,target} - C_{t,actin})_{negative\ control}$. Each set of experiments was repeated independently three times using larvae collected from separate genetic crosses.

Isothermal Titration Calorimetry. ITC measurements were performed at 25 °C on a MicroCal VP-ITC (MicroCal, Inc., Northampton, MA). A standard experiment consisted of titrating 10 μL of a 500 μM ligand solution from a 250 μL syringe (rotating at 300 rpm) into a sample cell containing 1.42 mL of a 10 μM DNA or RNA solution. An ITC experiment consisted of 28 total injections (first injection was 5 μL, subsequent injections were 10 μL), with a 10 s duration per injection and delay of 380 s between injections. The initial delay prior to the first injection was 300 s. To derive the heat associated with each injection, the area under each isotherm (microcalories per second versus seconds) was determined by integration by the graphing program Origin 7.0 (MicroCal, Inc. Northampton, MA). The first data point from each ITC experiment was omitted when fitting to binding models due to possible diffusive mixing of material near the tip of the syringe. The fitting requirements were such that the thermodynamic parameters were derived from curves that produced the lowest amount of deviation. In most cases, fitting to a sequential site-binding/model-binding sites gave the most accurate data. The ligand stock solution was 10 mM in water. Double-stranded and hairpin DNA or RNA solutions were freshly prepared by mixing required volumes of the corresponding single-stranded oligomers and annealing by heating in a water bath at >90 °C for 5 min and slowly cooling to room temperature. MOPS buffer solution (1 M), NaCl solution (5 M), and biological grade water were added to make up an oligonucleotide solution with 20 mM MOPS (pH 7.0 ± 0.2), 300 mM NaCl.

■ ASSOCIATED CONTENT

Supporting Information

The Supporting Information is available free of charge on the ACS Publications website at DOI: 10.1021/jacs.5b09266.

Synthesis of intermediates and other ligands, NMR spectra and HPLC chromatograms of ligands tested in cellular experiments, protocols and more data of CUG^{exp} level experiments, molecular modeling, reverse titration and ITC binding study, MALDI experiments, *in vitro* cleavage and transcription assays, confocal microscopy and *IR* splicing experiments, fly experiments of ligands at different doses and the controls (PDF)

Description of the supporting movie (PDF)

Progression of larvae crawling (MOV)

■ AUTHOR INFORMATION

Corresponding Author

*sczimmer@illinois.edu

Notes

The authors declare no competing financial interest.

■ ACKNOWLEDGMENTS

This work was supported by the National Institutes of Health (RO1AR058361) and the Muscular Dystrophy Association (295229). We thank Auinash Kalsotra (University of Illinois, Urbana—Champaign, IL) for the GFP-DT0 and GFP-DT960 plasmids, Thomas Cooper (Baylor College of Medicine, Houston, Texas) for the DT960 minigene plasmid, Maurice Swanson (University of Florida, Gainesville, FL) for the $(CTG)_{74}$ plasmid, and Nicholas Webster (University of California, San Diego) for the *IR* minigene plasmid.

■ REFERENCES

(1) Kunnumakkara, A. B.; Anand, P.; Aggarwal, B. B. *Cancer Lett.* **2008**, *269*, 199−225.

(2) Imming, P.; Sinning, C.; Meyer, A. *Nat. Rev. Drug Discovery* **2006**, *5*, 821−834.

(3) Anighoro, A.; Bajorath, J.; Rastelli, G. *J. Med. Chem.* **2014**, *57*, 7874−7887.

(4) Morphy, R.; Rankovic, Z. *J. Med. Chem.* **2005**, *48*, 6523−6543.

(5) Meunier, B. *Acc. Chem. Res.* **2008**, *41*, 69−77.

(6) Gatchel, J. R.; Zoghbi, H. Y. *Nat. Rev. Genet.* **2005**, *6*, 743−755.

(7) Wheeler, T. M.; Sobczak, K.; Lueck, J. D.; Osborne, R. J.; Lin, X.; Dirksen, R. T.; Thornton, C. A. *Science* **2009**, *325*, 336−339.

(8) Gareiss, P. C.; Sobczak, K.; McNaughton, B. R.; Palde, P. B.; Thornton, C. A.; Miller, B. L. *J. Am. Chem. Soc.* **2008**, *130*, 16254−16261.

(9) Warf, M. B.; Nakamori, M.; Matthys, C. M.; Thornton, C. A.; Berglund, J. A. *Proc. Natl. Acad. Sci. U. S. A.* **2009**, *106*, 18551−18556.

(10) Parkesh, R.; Childs-Disney, J. L.; Nakamori, M.; Kumar, A.; Wang, E.; Wang, T.; Hoskins, J.; Tran, T.; Housman, D.; Thornton, C. A.; Disney, M. D. *J. Am. Chem. Soc.* **2012**, *134*, 4731−4742.

(11) Arambula, J. F.; Ramisetty, S. R.; Baranger, A. M.; Zimmerman, S. C. *Proc. Natl. Acad. Sci. U. S. A.* **2009**, *106*, 16068−16073.

(12) Wong, C.-H.; Nguyen, L.; Peh, J.; Luu, L. M.; Sanchez, J. S.; Richardson, S. L.; Tuccinardi, T.; Tsoi, H.; Chan, W. Y.; Chan, H. Y. E.; Baranger, A. M.; Hergenrother, P. J.; Zimmerman, S. C. *J. Am. Chem. Soc.* **2014**, *136*, 6355−6361.

(13) García-López, A.; Llamusí, B.; Orzáez, M.; Pérez-Payá, E.; Artero, R. D. *Proc. Natl. Acad. Sci. U. S. A.* **2011**, *108*, 11866−11871.

(14) Jahromi, A. H.; Honda, M.; Zimmerman, S. C.; Spies, M. *Nucleic Acids Res.* **2013**, *41*, 6687−6697.

(15) Cho, D. H.; Thienes, C. P.; Mahoney, S. E.; Analau, E.; Filippova, G. N.; Tapscott, S. J. *Mol. Cell* **2005**, *20*, 483−489.

(16) Moseley, M. L.; Zu, T.; Ikeda, Y.; Gao, W.; Mosemiller, A. K.; Daughters, R. S.; Chen, G.; Weatherspoon, M. R.; Clark, H. B.; Ebner, T. J.; Day, J. W.; Ranum, L. P. W. *Nat. Genet.* **2006**, *38*, 758−769.

(17) Zu, T.; Gibbens, B.; Doty, N. S.; Gomes-Pereira, M.; Huguet, A.; Stone, M. D.; Margolis, J.; Peterson, M.; Markowski, T. W.; Ingram, M. A. C.; Nan, Z.; Forster, C.; Low, W. C.; Schoser, B.; Somia, N. V.; Clark, H. B.; Schmechel, S.; Bitterman, P. B.; Gourdon, G.; Swanson, M. S.; Moseley, M.; Ranum, L. P. W. *Proc. Natl. Acad. Sci. U. S. A.* **2011**, *108*, 260−265.

(18) Wojciechowska, M.; Olejniczak, M.; Galka-Marciniak, P.; Jazurek, M.; Krzyzosiak, W. J. *Nucleic Acids Res.* **2014**, *42*, 11849−11864.

(19) Kalsotra, A.; Singh, R. K.; Gurha, P.; Ward, A. J.; Creighton, C. J.; Cooper, T. A. *Cell Rep.* **2014**, *6*, 336−345.

(20) Laurent, F. X.; Sureau, A.; Klein, A. F.; Trouslard, F.; Gasnier, E.; Furling, D.; Marie, J. *Nucleic Acids Res.* **2012**, *40*, 3159−3171.

(21) Pettersson, O. J.; Aagaard, L.; Andrejeva, D.; Thomsen, R.; Jensen, T. G.; Damgaard, C. K. *Nucleic Acids Res.* **2014**, *42*, 7186−7200.

(22) Lee, J. E.; Bennett, C. F.; Cooper, T. A. *Proc. Natl. Acad. Sci. U. S. A.* **2012**, *109*, 4221−4226.

(23) Wheeler, T. M.; Leger, A. J.; Pandey, S. K.; MacLeod, A. R.; Nakamori, M.; Cheng, S. H.; Wentworth, B. M.; Bennett, C. F.; Thornton, C. A. *Nature* **2012**, *488*, 111−115.

DOI: 10.1021/jacs.5b09266
J. Am. Chem. Soc. 2015, 137, 14180−14189

(24) Guan, L.; Disney, M. D. *Angew. Chem., Int. Ed.* **2013**, *52*, 1462−1465.
(25) Coonrod, L. A.; Nakamori, M.; Wang, W.; Carrell, S.; Hilton, C. L.; Bodner, M. J.; Siboni, R. B.; Docter, A. G.; Haley, M. M.; Thornton, C. A.; Berglund, J. A. *ACS Chem. Biol.* **2013**, *8*, 2528−2537.
(26) Wong, C.-H.; Richardson, S. L.; Ho, Y.-J.; Lucas, A. M. H.; Tuccinardi, T.; Baranger, A. M.; Zimmerman, S. C. *ChemBioChem* **2012**, *13*, 2505−2509.
(27) Jahromi, A. H.; Nguyen, L.; Fu, Y.; Miller, K. A.; Baranger, A. M.; Zimmerman, S. C. *ACS Chem. Biol.* **2013**, *8*, 1037−1043.
(28) Palmer, A. J.; Wallace, H. M. *Amino Acids* **2010**, *38*, 415−422.
(29) Trawick, B. N.; Daniher, A. T.; Bashkin, J. K. *Chem. Rev.* **1998**, *98*, 939−960.
(30) Lönnberg, H. *Org. Biomol. Chem.* **2011**, *9*, 1687−1703.
(31) Breslow, R.; Huang, D. L.; Anslyn, E. *Proc. Natl. Acad. Sci. U. S. A.* **1989**, *86*, 1746−1750.
(32) Miller, J. W.; Urbinati, C. R.; Teng-Umnuay, P.; Stenberg, M. G.; Byrne, B. J.; Thornton, C. A.; Swanson, M. S. *EMBO J.* **2000**, *19*, 4439−4448.
(33) Wong, C. H.; Fu, Y.; Ramisetty, S. R.; Baranger, A. M.; Zimmerman, S. C. *Nucleic Acids Res.* **2011**, *39*, 8881−8890.
(34) Savkur, R. S.; Philips, A. V.; Cooper, T. A. *Nat. Genet.* **2001**, *29*, 40−47.
(35) Lanson, N. A.; Maltare, A.; King, H.; Smith, R.; Kim, J. H.; Taylor, J. P.; Lloyd, T. E.; Pandey, U. B. *Hum. Mol. Genet.* **2011**, *20*, 2510−2523.
(36) Nichols, C. D.; Becnel, J.; Pandey, U. B. *J. Visualized Exp.* **2012**, *61*, e3795.
(37) Batlevi, Y.; Martin, D. N.; Pandey, U. B.; Simon, C. R.; Powers, C. M.; Taylor, J. P.; Baehrecke, E. H. *Proc. Natl. Acad. Sci. U. S. A.* **2010**, *107*, 742−747.
(38) Schmittgen, T. D.; Livak, K. J. *Nat. Protoc.* **2008**, *3*, 1101−1108.
(39) Garcia-Lopez, A.; Monferrer, L.; Garcia-Alcover, I. *PLoS One* **2008**, *3*, e1595.
(40) Garcia-Alcover, I.; Colonques-Bellmunt, J.; Garijo, R.; Tormo, J. R.; Artero, R.; Álvarez-Abril, M. C.; López Castel, A.; Pérez-Alonso, M. *Dis. Models & Mech.* **2014**, *7*, 1297−1306.
(41) Freeman, M. *Cell* **1996**, *87*, 651−660.
(42) Brand, A. H.; Perrimon, N. *Development* **1993**, *118*, 401−415.

DOI: 10.1021/jacs.5b09266
J. Am. Chem. Soc. 2015, 137, 14180−14189